Metallophysics and Advanced Technologies
Металофіз. новітні технол.
Metallofiz. Noveishie Tekhnol.
2024, vol. 46, No. 6, pp. 531–547
https://doi.org/10.15407/mfint.46.06.0531
Reprints available directly from the publisher

PACS numbers: 63.20.D-, 63.20.kp, 63.22.Np, 65.40.Ba, 65.40.gd, 68.65.-k, 81.05.Zx

Vibration Dynamics of the Ordered Bimetallic Surface Alloy System Pt(110)–(2×1)Cu

N. Laouici[*], E. Sakher[*,**], R. Tigrine[*,***],R. Chadli[***], and S. Bouchareb[*]

[*]*Université Ahmed Draia,*
6 Nationale Route,
1000 Adrar, Algeria
[**]*Environmental Research Centre,*
Boughazi Saïd Ave.,
23000 Annaba, Algeria
[***]*Laboratoire de Physique et Chimie Quantique,*
Université Mouloud Mammeri de Tizi-Ouzou,
B.P. 17 RP,
15000 Tizi-Ouzou, Algeria

In the present investigation, we examine systematically the dynamical behaviour of the architecturally complex bimetallic surface alloy, namely, Pt(110)–(2×1)Cu, which is characterized by a half-monolayer (0.5 ML) of copper atoms deposited on a platinum (110) substrate. By leveraging Newtonian mechanics within the harmonic approximation, we construct the dynamic matrix pertinent to the bulk material. The extraction of eigenvalues and eigenvectors is pivotal in formulating a robust theoretical framework, anchored in the Green's function approach explicitly designed for our model system. Utilizing this sophisticated theoretical model, we are able to elucidate the phonon dispersion relationships traversing the high-symmetry pathways ΓY, YS, SX, and $X\Gamma$ of the surface Brillouin zone, as well as deduce the associated local vibrational densities of states. An extensive interpretation of the computational results reveals a notable phenomenon, namely, the electron redistribution between the platinum and copper atoms within the alloy interface, which, in turn, altered the interfacial force constants. This electron redistribution

Corresponding author: Nourelhouda Laouici
E-mail: nou.laouici@univ-adrar.edu.dz

Citation: N. Laouici, E. Sakher, R. Tigrine,R. Chadli, and S. Bouchareb, Vibration Dynamics of the Ordered Bimetallic Surface Alloy System Pt(110)–(2×1)Cu, *Metallofiz. Noveishie Tekhnol.*, **46**, No. 6: 531–547 (2024).
DOI: 10.15407/mfint.46.06.0531

prompts significant divergences in the vibrational density of states at the individual platinum and copper atomic sites at the Cu/Pt(110) juncture, as opposed to the undisturbed Pt(110) surface, suggesting potential pathways for innovative platinum-catalysed surface reactions. Furthermore, our research delineates the variation of several thermodynamic properties as a function of surface composition and thermal parameters, which may offer insights into the stability and reactivity of such bimetallic surfaces.

Key words: alloyed surfaces, phonon surface properties, vibrational density of states, eigenvalue matching techniques, Green's function methods.

В статті систематично досліджено динамічну поведінку складного біметалевого приповерхневого стопу Pt(110)–(2×1)Cu, який складається з пів моношару (0,5 ML) міді, нанесеного на платинову (110) підкладинку. На основі використання класичної механіки в рамках гармонічного наближення побудовано динамічну матрицю для об'ємного матеріялу. Знаходження власних значень і власних векторів є ключовим для створення надійної теоретичної основи, заснованої на методі Ґрінових функцій, знайдених явно для нашої модельної системи. Використовуючи цей теоретичний модель, можна знайти фононні дисперсійні співвідношення для високосиметрійних напрямків ΓY, YS, SX і XΓ Бріллюенової зони, а також розрахувати відповідні локальні густини коливних станів. Аналіза результатів обчислень показала, що перерозподіл електронів між атомами Платини та Купруму на інтерфейсі приводить до зміни міжфазних силових констант. Цей перерозподіл електронів зумовлює істотну ріжницю між густинами коливних станів для окремих атомів Платини та Купруму на контакті Cu/Pt(110) та для поверхні Pt(110), що вказує на потенційні шляхи для реалізації каталізованої платиною поверхневої реакції. Крім того, встановлено, що термодинамічні властивості досліджуваної системи залежать від складу поверхні та теплових параметрів, що може пояснити стабільність і реакційну здатність таких біметалевих поверхонь.

Ключові слова: леґовані поверхні, фононні властивості поверхні, густина коливних станів, методи знаходження власних значень, метод Ґрінових функцій.

(Received 4 December, 2023; in final version, 25 December, 2023)

1. INTRODUCTION

In recent years, there has been an uptick in both theoretical and experimental studies focusing on the stability and dynamics of both ordered and disordered alloy surfaces [1–6]. The intrigue surrounding these surfaces stems from their diverse applications in myriad technological arenas, from novel catalyst and sensor development to surface corrosion protection [7, 8]. One can achieve alloyed surface configurations by overlaying one metal onto a precisely defined monocrystalline face of another. Post heat treatment and apt annealing, which facilitate the dissolution of both metals, various surface alloy configurations emerge [9]. It is crucial to highlight that the fabrication and detailed analysis of these bimetallic interfaces and definitive surface alloys, especially in rigorous vacuum environments, have become feasible due to cutting-edge surface diagnostic techniques [10]. Of particular interest are bimetal pairings that feature platinum. These alloys have garnered substantial interest given their promise in catalytic applications. Notably, copper, when interfaced with a Pt substrate, showcases heightened catalytic prowess in the oxygenation reaction, outperforming the pure Pt(110) surface [11, 12]. Various alloying schemes involving Pt and Cu have been commercialized as catalysts in hydrogenation processes [13].

The Pt(110) substrate has also been the focal point of extensive research, indicative of the genesis of the Pt(110)–(2×1)Cu surface reconformation alloy upon Cu monolayer deposition, peaking at 830 K, resulting from the substitution of Cu adatoms on the platinum substrate's exterior layer [14–16]. However, investigations centred on (110) faces have been scantier, given the more complex growth dynamics associated with copper deposition on this face [17]. Tunnelling electron microscopy has emerged as a potent modality to probe the deposition-induced growth dynamics and topological attributes of these surfaces [18, 19].

The existence of such interfaces is pivotal in both catalytic activities and crystalline propagation. Structural anomalies have been identified as chemically receptive zones, favoured for uptake by various atomic and molecular species. Depending on the extant conditions, these can either catalyse or inhibit surface-bound reactions. To decode the energy interplay in these phenomena, elucidating the vibrational mode landscape on the interface is paramount. Motivated by this, our study seeks to determine the vibrational dynamics of the surface alloy Pt(110)–(2×1)Cu, stemming from varying Cu concentrations on a Pt(110) substrate.

To our understanding, no prior work has ventured into the vibrational dynamics of the Cu/Pt(110) interface. This alloyed configuration is depicted in Fig. 1. Predominantly, research efforts have been channelled towards pure platinum (110) surfaces and reconformed surfaces of other metallic entities.

Our manuscript is structured as follows: Sec. 2 elucidates the matching formalism tailored for our generalized model, aimed at ascertaining surface-specific phonons and boundary vibrational spectra; Subsec. 2.1 operationalizes this theoretical framework to compute surface phonons for the Cu/Pt(110) ordered alloy, termed Pt(110)–(2×1)Cu; herein, we also furnish our vibrational calculations for Cu, both in bulk and on the surface, for benchmarking, showcasing a congruence with extant experimental and theoretical findings; Sec. 3 harnesses this model to derive the localized vibrational densities of states at the Pt and Cu sites on the alloyed interface. We conclude with Sec. 4,

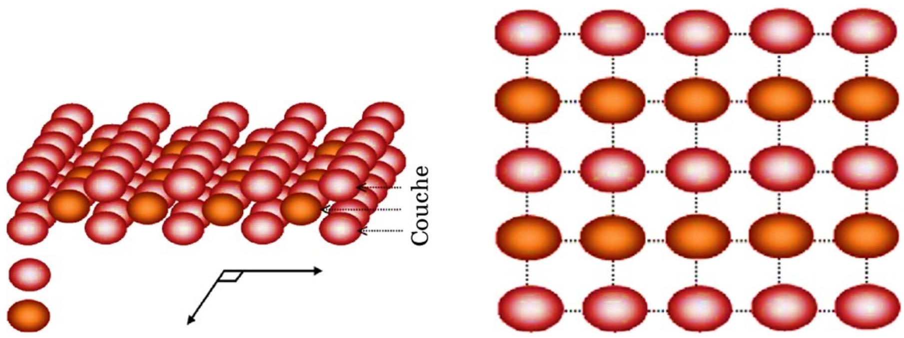

Fig. 1. Schematic representation of the ordered surface alloy Pt(110)–(2×1)Cu: model of Cu atoms deposited on the Pt(110) substrate (*a*), detailed view of the first atomic layer highlighting Cu atoms (denoted by heavy shaded (brown) circles) and Pt atoms (denoted by light shaded (grey) circles) (*b*).

offering overarching takeaways.

2. THEORETICAL APPROACH

The imposition of a boundary surface within an infinite semi-solid medium induces a defect, thereby, perturbing the translational symmetry along the axis orthogonal to this boundary. This perturbation gives rise to a complex relationship governing the vibrational amplitudes of constituent atoms along Cartesian axes. Specifically, this relationship manifests between an atom situated within a discrete crystalline plane p, and another within a disparate but parallel plane p', both congruent with respect to the surface yet embedded in the solid's volumetric confines. The ensuing co-ordination relationship is critical for the mathematical description of this system:

$$u_\alpha(l', p', \omega) = u_\alpha(l, p, \omega) z^{(p'-p)} e^{i\mathbf{qr}(l,l')}. \tag{1}$$

Within this framework, the term z denotes a phase factor, which is predicted to be oriented normal to the metallic interface, subject to the constraint $|z| \leq 1$. Concurrently, q represents a wave vector situated within the confines of the first Brillouin zone. Additionally, α serves as an identifier for one of the Cartesian coordinates, namely x, y, or z. Upon integrating Eq. (1) into the equation of motion, a comprehensive system of linear equations is formulated for the displacement vectors at the atomic lattice points within the volumetric matrix. These vectors, denoted by $|u\rangle$, encompass the displacement vectors $|u_\alpha(l, \omega)\rangle$ for each atomic site within the elementary lattice. This system is succinctly expressible in a matrix notation, encapsulating the intricate interplay between the atomic displacements and the lattice dynamics. The mathematical expression of this relationship can be succinctly captured as follows:

$$(\Omega^2 I - M(\varphi_x, \varphi_y, \zeta, \lambda)) = |0\rangle . \quad (2)$$

In this analytical context, the variables φ_x and φ_y are delineated through their dependence on q_x and q_y, which represent the components of the wave vector **q** along the Cartesian co-ordinates x and y within the reciprocal lattice framework. The scalar λ is introduced as a descriptor of the interatomic force constants, encompassing interactions between both nearest and next-nearest neighbours within the crystalline array.

The normalized frequency Ω is defined as the ratio of the frequency ω to a characteristic frequency ω_0 of the bulk material, where ω_0 is determined by the equation $\omega_0^2 = K_1 / M_l$. Here, K_1 symbolizes the force constant governing the interactions among the first neighbours in the flawless region of the bulk, and M_l represents the atomic mass.

The matrix-system compatibility condition unlocks the possibility of deriving a polynomial equation for each $(\mathbf{q}, \Omega)$ pair, the solutions of which delineate distinct vibrational modes within the bulk that are normal to the metallic boundary. Propagative modes are those for which $|z| = 1$, whereas evanescent modes, which decay from the surface into the bulk, satisfy the condition $|z| < 1$.

The preliminary step in discerning phonon states localized proximate to a planar metallic interface with imperfections within a semi-infinite solid mandates the calculation of these evanescent modes in the $(\mathbf{q}, \Omega)$ space. Following this, the equations governing vibrational movements, as stipulated by Eq. (2), are ascertained for atoms situated at strategic locations within the three delineated regions. This culminates in the formulation of a non-square matrix equation system, denoted by M_d, where the quantity of equations is less than the number of unknown atomic displacements.

To resolve such an equation system, it is requisite to condense the number of indeterminatenesses, thereby, fabricating a homogeneous set of linear equations. For each collected data set $(\mathbf{q}, \Omega)$, the atomic displacements are characterized by evanescent modes, which are portrayed as a linear superposition of n vibrational modes derived from the comprehensive bulk dynamics investigation, oriented normally to the metallic interface. These n modes correspond to the z roots meeting the criterion $|z| < 1$. Thus, the displacement at each atomic site is formulated by the ensuing relationship, which is yet to be explicitly defined in the equation

$$u_\alpha(l, \omega) = \sum_{\upsilon=1}^{n} z_\nu^{p-p'} A(\alpha, \nu) R_\nu . \quad (3)$$

In this model, u_α denotes the amplitude of vibrational displacement parallel to the Cartesian axis α, with p being the third spatial co-ordinate of an atom l, which conforms to the condition $p \geq p_s$ and, here, represents the third co-ordinate of the planar surface. The index α encapsulates the three Cartesian axes: x, y, and z. The symbol n signifies the count of evanescent modes, which are determined through the analysis of bulk dynamics. Moreover, R_ν is a unit vector that characterizes the ν-th evanescent mode within the set $\{R\}$, and z_ν is the phase factor associated with the ν-th evanescent mode as derived from the dynamic matrix in the bulk material. The coefficient $A(\alpha, \nu)$ quantifies the weighted contribution of the ν-th evanescent mode in the direction of α.

The simultaneous resolution of the phase factors z_ν, which define the evanescent modes, and the pertinent eigenvectors that emanate from the bulk dynamic analysis, facilitates the construction of a corresponding matrix, henceforth indicated as M_R as per the elaborations in Refs. [20, 25]. The product of the matrices M_d and M_R, as previously defined, culminates in the formation of a square matrix M_S. This matrix characterizes a homogeneous system of equations where non-trivial solutions can be derived, indicating the presence of non-zero vibrational states within the system. These solutions are instrumental in describing the behaviour of evanescent modes and their contributions to the overall vibrational characteristics of the material, particularly in regions proximate to structural defects or surfaces:

$$\det(\Omega^2 I - M_S(\varphi_x, \varphi_y, \zeta, \lambda)) = 0\,. \tag{4}$$

This equation facilitates the identification of vibrational modes localized in proximity to the metallic surface. Consequently, it becomes feasible to compute the dispersion branches of localized phonons and other metallic surface properties.

2.1. Localized States of Clean Surface

The manifestation of a surface within a solid medium induces significant modifications to the interatomic bonding configurations, particularly within the surface immediate atomic strata. These alterations exert a profound impact on the vibrational attributes of the atoms in close proximity to the surface, leading to behaviours distinct from those in the homogenous bulk material. It is therefore of paramount importance to conduct a meticulous investigation of the vibrational properties of atoms within these surface layers, as they play a crucial role in phenomena such as adsorption, scattering, and crystal growth processes at the surface. The study of lattice dynamics at the surface is an essential tool for elucidating the physical properties of surfaces and complements other surface analyses concerning structural and electronic properties.

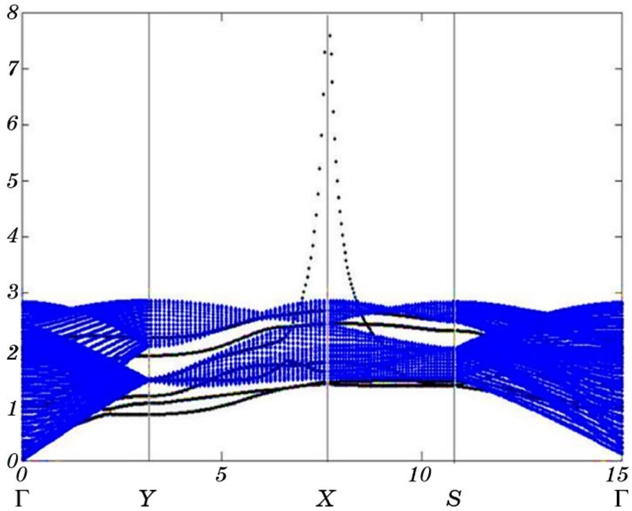

Fig. 2. Calculated surface phonon and resonance dispersion for the Pt(110) clean surface, indicated by the black curves. The shaded regions represent the projected bulk phonon bands.

The impetus for such studies is derived from the extensive applications that these surfaces find across various technological fields. This includes the development of novel catalysts, sensors, and materials designed to mitigate corrosion. The presence of the surface introduces a disruption in symmetry along the vertical z-axis, leading to the manifestation of localized states, which are absent in the bulk. The multiplicity of these localized vibrational modes is intrinsically linked to the nature of the surface irregularity, and is directly influenced by the size of the defect matrix, which is obtained from the application of Newton's equations at the surface inaugural layers.

Advancements in experimental techniques, particularly inelastic electron tunnelling spectroscopy (IETS), have provided a powerful means to assay surface phonons with high precision. These methodologies permit the measurement of surface vibrations across a broad energy range, encompassing all wave vectors within the Brillouin zone. Such capabilities have significantly enhanced our ability to derive accurate surface phonon dispersion curves (Fig. 2), thereby, deepening our understanding of surface dynamics.

2.2. Dynamic Properties of Surface Alloys

In the current analysis, we conduct an in-depth examination of the dynamical attributes of the Pt(110)–(2×1)Cu metal alloy surface system, employing the application of Eq. (4) as the theoretical underpinning.

Our primary objective is to ascertain the characteristics of surface phonons pertaining to the pristine Pt(110) surface, which we employ as a baseline reference. This comparative approach allows us to quantify rigorously the influence that copper atom incorporation exerts on the vibrational landscape of the surface. The computed phonon spectra, designated by dotted lines in our graphical representations, encompass both the unalloyed Cu(110) surface and the bimetallic Pt(110)–(2×1)Cu alloy surface. These spectra are mapped along the principal symmetry vectors of the surface Brillouin zone, specifically along the pathways ΓY, YS, SX, and $X\Gamma$, as delineated in Fig. 3. This methodology enables a meticulous delineation of the modifications induced by the copper deposition, thereby enhancing our comprehension of the altered vibrational dynamics within the bimetallic surface system.

Within this study, the findings are contextualized through the lens of interatomic bond lengths between specific atomic sites. Precisely, leveraging the computational framework of our model, we ascertain the force constants corresponding to the bond lengths of both nearest neighbour interactions—denominated as $(\mathrm{Cu–Cu})^1$, $(\mathrm{Pt–Pt})^1$, $(\mathrm{Cu–Pt})^1$—and next-nearest neighbour interactions—$(\mathrm{Cu–Cu})^2$, $(\mathrm{Pt–Pt})^2$, $(\mathrm{Cu–Pt})^2$. The determination of these bond lengths is grounded in the optimized atomic positions at the interfacial boundary of the Cu/Pt (110) surface alloy. The calculated force constants, which are fundamental to the vibrational properties of the surface, are systematically compiled and presented in Table 1. This data serves as a crucial element for the in-depth analysis of the mechanical stability and dynamical be-

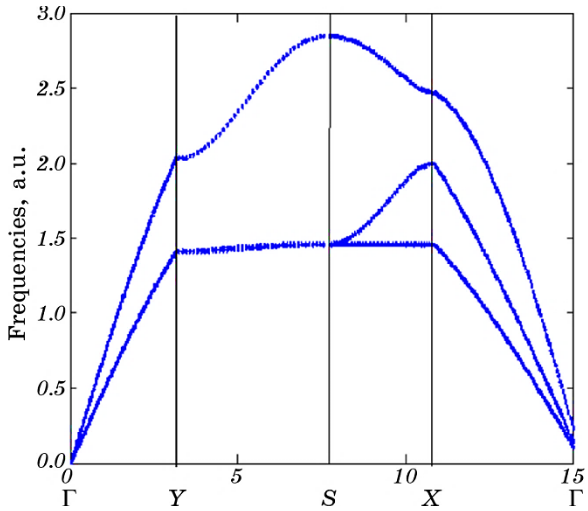

Fig. 3. Calculated phonon dispersion curve for bulk Pt following the directions of high symmetry in the f.c.c. crystal.

haviour of the surface structure under investigation.

As a fundamental step in our verification process, we conducted calculations of the phonon dispersion curves for bulk platinum, utilizing the (Pt–Pt)^1 and (Pt–Pt)^2 force constants delineated in Table 1. These calculations traverse the high-symmetry vectors of the platinum Brillouin zone (BZ). The graphical depiction of these phonon dispersion curves is presented in Fig. 4. In the analysis of the Δ direction within the BZ, our computations revealed the presence of two distinct acoustic phonon branches: transverse (T) and longitudinal (L), a pattern that is replicated along the Λ direction. Notably, at the high symmetry point X, we observe a degeneration of the transverse acoustic phonon mode, which bifurcates into two separate modes.

TABLE 1. Interatomic distances and transferable force constants for an f.c.c. bulk copper unit cell: assignment of the nearest and next-nearest neighbours' distances and empirical determination of force constants as a function of bond lengths [49].

Pair type	Bond length, Å	Force constants, J/m^2
(Cu–Cu)^1	2.566	27.5
(Cu–Cu)^2	3.615	1.4
(Pt–Pt)^1	3.28	35.24
(Pt–Pt)^2	3.77	1.203
(Cu–Pt)^1	2.67	28.64
(Cu–Pt)^2	3.77	1.02

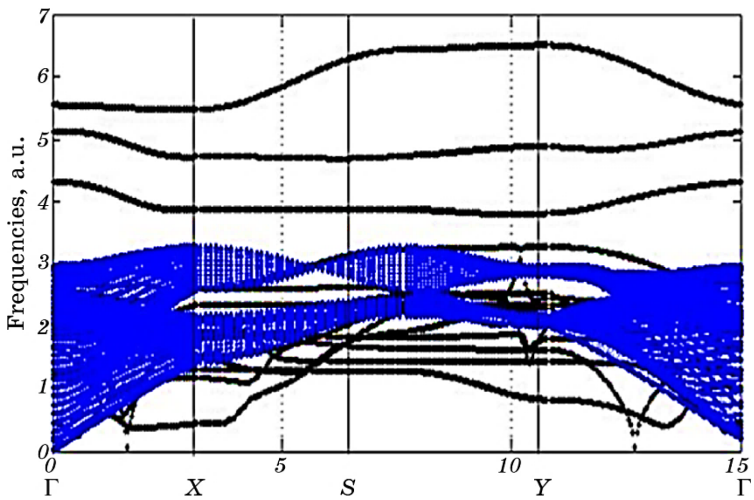

Fig. 4. Calculated surface phonon and resonance dispersion for the Pt(110)–(2×1)Cu surface alloy, indicated by the black curves. The shaded regions represent the projected bulk phonon bands.

Further examination along the Σ direction unveils three acoustic phonon branches: a single longitudinal (L) and two transverse (T_1 and T_2) branches. The results from these comprehensive analyses exhibit a consistent concordance with the spectrum of findings reported in both experimental and theoretical studies conducted by other researchers, as referenced in [26–31].

Expanding upon these investigations, the surface phonon spectra and associated resonances for the structured-surface alloy system Pt(110)–(2×1)Cu were calculated across the high-symmetry directions in the two-dimensional BZ. These trajectories include $\bar{\Gamma}\bar{Y}$, $\bar{Y}\bar{S}$, $\bar{S}\bar{X}$, $\bar{X}\bar{\Gamma}$, adhering to the comprehensive theoretical framework outlined in Sec. 2. The outcomes of these intricate computations are illustrated in Fig. 3. The phonon spectra of the surface alloy superstructure are characterized by a distinct count and arrangement of surface vibrational modes. These modes embody a fusion of individual branches coalescing surface phonons and resonances both external to and within the confines of the projected bulk phonon bands, respectively.

3. VIBRATIONAL DENSITY OF STATE OF THE SURFACE AND SURFACE ALLOY

The spectral densities, along with the state densities related to various modes proximal to the surface, can be articulated through the following generalized equation:

$$D_s(\Omega) = \sum_{\varphi_y} \sum_{p\alpha} \zeta^{(p,p)}_{(\alpha,\alpha)}(\varphi_y, \Omega) = -\frac{2\Omega}{\pi} \sum_{\varphi_\alpha} \sum_{p,\alpha} \lim_{\varepsilon \to 0} (\operatorname{Im} G^{pp}_{\alpha\alpha}(\varphi_y, \Omega + i\varepsilon)) . \qquad (5)$$

Elastic excitations are known to be the progenitors of a multitude of intriguing physical properties, which can be elucidated through the computational analysis of the vibrational state density [32]. It is observed that the state density per atomic layer begins to converge with the volumetric state density from the fourth layer onwards, presenting only marginal deviations. The most pronounced differences when compared to the bulk are observed within the inaugural Pt atomic layer and the subsequent Pt–Cu intermixed layer.

Figure 6, *a–f* present correspondingly our calculated density of states (DOS) results for the defined considered surface alloys, namely Pt(110)–(2×1)Cu. In each of these figures, we also present the normalized spectra (dotted) on the same scale, for the DOS of the equivalent Cu atomic sites for the Pt(110) surface boundary of the pure Cu crystal.

In our investigations, we have meticulously computed the phonon state densities for the Cu and Pt atoms within the alloyed layer, treating each species discretely. The vibrational modes associated with atomic displacements in the Pt–Cu alloy layer exhibit a widespread

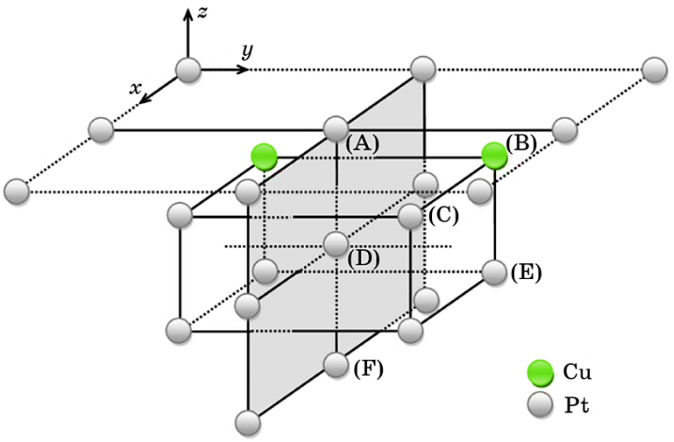

Fig. 5. Schematic analysis of atomic density in Pt(110)–(2×1)Cu alloy surface [32].

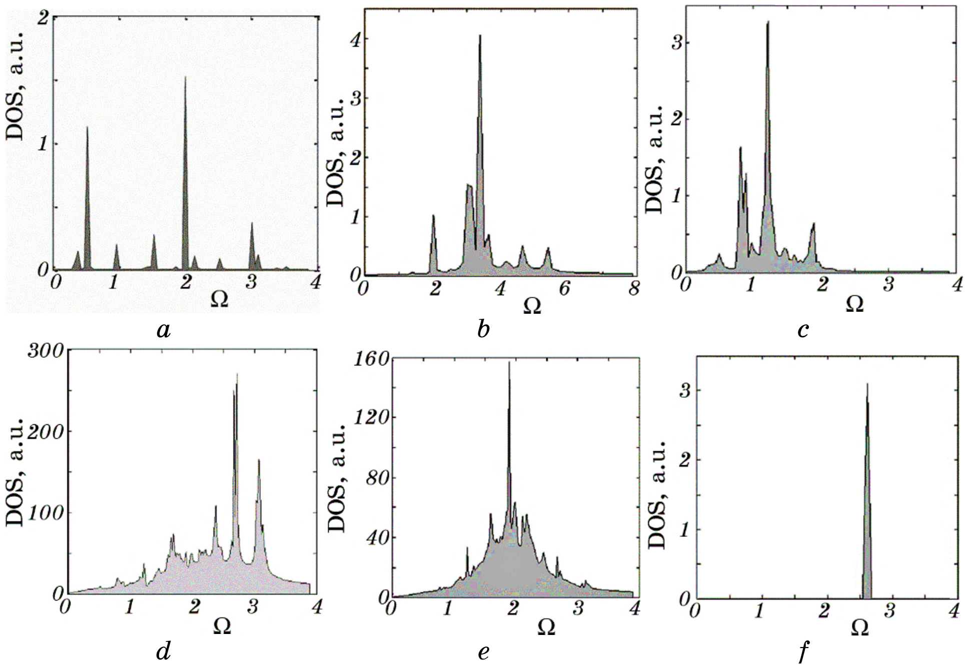

Fig. 6. Densities of vibrational states of the sites belonging to the interface Pt–Cu: state density of atoms (*a*), (*b*), (*c*), (*d*), (*e*) and (*f*) in perturbed zone.

distribution, extending from lower frequency domains to higher energy thresholds, as evidenced by the multifarious peaks present in the state density spectra of both atomic types.

A particularly notable feature within the vibrational state density spectra for the Pt–Cu alloy is the prevalence of peaks associated with Cu atom displacements over those associated with Pt atom displacements. This observation corroborates the presence of new phonon branches within the dispersion curves (illustrated in Fig. 3) for the structured Pt(110)–(2×1)Cu alloy surface, predominantly originating from the copper atom vibrations perpendicular to the Pt–Cu interfacial plane. The root of this disparity in vibrational contributions stems from the significant mass differential between Cu and Pt atoms.

In contrast, a conspicuous aspect of the vibrational state density spectra for the ordered Pt(110)–(2×1)Cu surface alloy is the manifestation of Cu-related vibrational peaks at frequencies lower than those of the bulk state densities, with these Cu peaks occurring at reduced frequencies relative to their Pt counterparts, particularly near the transverse bands in the bulk. The most prominent peaks in the first layer correlate with vibrations of the outermost platinum layer in a direction orthogonal to the surface.

The calculated local vibrational DOS for each constituent atom offers distinctive local fingerprints for the surface alloys in question. These DOS calculations are instrumental for the subsequent derivation of all pertinent thermodynamic properties for the systems under study, utilizing the partition function framed within the harmonic approximation of lattice dynamics. Within this context, the vibrational contributions to the free energy denoted as F emerge as a focal point of the investigation, providing insights into the energetic landscape of the surface alloys.

4. THERMODYNAMIC PROPERTIES

Phonons, rooted in the foundations of quantum mechanics and embodying the principle of wave–particle duality, exert a profound influence on a plethora of solid-state properties. These include critical thermal attributes such as vibrational specific heat [1, 2], vibrational free energy [33, 34], vibrational internal energy [1–3], and vibrational entropy [3–5]. Consequently, the theory of lattice vibrations becomes indispensable for the inclusion of phonon contributions in the computation of thermodynamic properties.

Within the realm of statistical physics, the partition function Z serves as a cornerstone concept that facilitates the deconvolution of the composite system into its harmonic oscillators. This leads to a scenario where the partition function manifests as the product of the individual partition functions corresponding to each vibrational mode [35, 36]. The expression for this pivotal function is articulated as follows:

$$Z = \sum_{n_{s(q)}} \exp(-E_{(q,s)} / k_B T). \tag{6}$$

The density of states is recognized as an exceptionally utilitarian metric in the realm of physics, not only for its direct measurability but also for its conceptualization as a continuous function in the context of the thermodynamic limit. This facilitates the calculation of a myriad of thermodynamic properties, contingent upon the computation of the vibrational density of states, thus, serving as a vital precursor to further thermodynamic inquiry [37, 38].

In the framework of thermodynamics, the total energy of a system, commonly referred to as the internal energy (U or E), particularly, within the volume, where the particle count is held constant to preserve unchanged energy levels, is intricately linked to and derivable from the partition function Z. The relationship between the internal energy and the partition function is not only fundamental but also quantifiable, allowing a robust method to compute the internal energy [37]:

$$U = \partial \ln Z / \partial\beta . \tag{7}$$

Considering the density of vibrational states $D(\omega)$, the internal energy U is transformed into the form [38]:

$$U_{\text{vib}} = k_B T \int_0^\infty \frac{h\omega}{k_B T} \operatorname{cth}\left(\frac{h\varpi}{k_B T}\right) D(\omega) d\omega . \tag{8}$$

The free energy F of a system can be expressed as:

$$F_{\text{vib}} = k_B T \int_0^\infty \ln(2 \operatorname{sh}(h\omega / (2k_B T)) D(\omega) d\omega . \tag{9}$$

The cohesive interrelation that seamlessly ties the free energy and internal energy in a thermodynamic system paves the way to unearth a pivotal thermodynamic quantity: the vibrational entropy denoted as S_{vib}. Mathematically, vibrational entropy is expounded as:

$$S_{\text{vib}} = k_B \int_0^\infty \left[\left(\frac{h\omega}{k_B T}\right) \operatorname{cth}\left(\frac{h\omega}{k_B T}\right) - \ln 2 \operatorname{sh}\left(\frac{h\omega}{2k_B T}\right) \right] D(\omega) d\omega . \tag{10}$$

Vibrational entropy is distinctively defined as a thermodynamic variable intrinsically associated with a system state of particulate constituents. Its quintessential role is to quantify the level of disorder or the extent of randomness present within a system. Embracing the postulate that entropy exists as a tangible attribute, particularly, in the analysis of a substantial aggregate of particles conceived as a continuum, we proceed to its quantification within the thermodynamic limit. The introduction of the vibrational density of states function $D(\omega)$

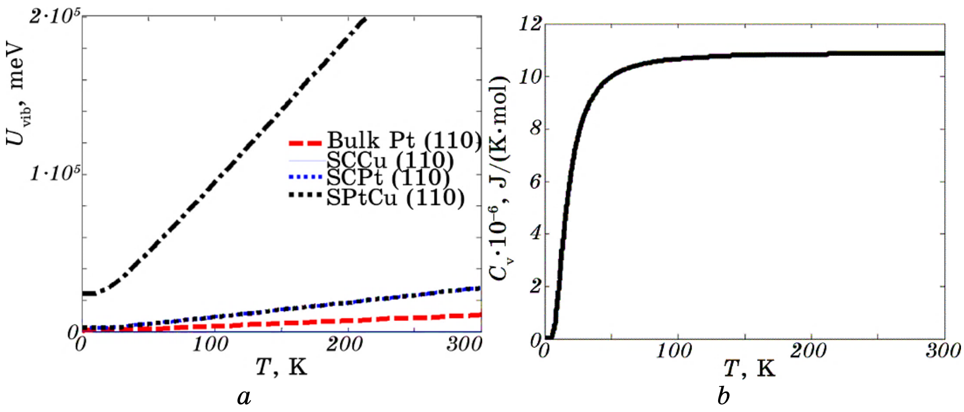

Fig. 7. Thermal properties of the material as a function of temperature: variation of internal energy U (a), changes in vibrational specific heat (b).

permits the establishment of an expression for vibrational entropy, providing a formulaic representation of this concept [38–41]:

$$S_{\text{vib}} = k_B \int_0^\infty \left[\left(\frac{h\omega}{k_B T} \right) \text{cth} \left(\frac{h\omega}{k_B T} \right) - \ln 2 \,\text{sh} \left(\frac{h\omega}{2k_B T} \right) \right] D(\omega) d\omega . \quad (11)$$

Specific heat, another essential material property, involves two primary forms of energy conduction in a solid: electronic and through atomic vibrations. Focusing on the phonon contribution (atomic vibration) and specifically the specific heat at constant volume due to its fundamental nature for solids, it is defined by [33–49]:

$$C_v = k_B \int_0^\infty \left[\left(\frac{h\omega}{k_B T} \right)^2 \text{sh}^{-2} \left(\frac{h\omega}{2k_B T} \right) \right] D(\omega) d\omega . \quad (12)$$

It is crucial to note that the vibrational specific heat encompasses the energy density variation associated with network vibrations as per temperature. The total system energy, encompassing the contributions of all particles within the system, is derived concerning the temperature T.

5. GENERAL CONCLUSIONS

This compendium delineates the outcomes from a comprehensive theoretical analysis of the vibrational phenomena within Cu/Pt(110) surface alloy systems, synthesized via the deposition of copper atoms upon a platinum (110) substrate. We have meticulously quantified and illustrated the dispersion branches of the surface phonons, resonances, and the vibrational density of states for the **Pt(110)–(2×1)Cu** surface alloys. These vibrational features serve as definitive indicators of the structural order and elucidate the unique elastic properties intrinsic to these alloys. The resonance of our results with extant theoretical constructs and empirical data underscores the efficacy of our methodology in predicting the thermophysical properties of these alloys.

Phonons are collective excitations representing lattice vibrations, with surface phonons specifically denoting the vibrational modes that are localized to surface structures, arising due to the periodicity, symmetry, and truncation of the bulk crystal lattice at the solid interface. The exploration of surface phonons is imperative for understanding the structural configuration and distinctive properties of surfaces, which often exhibit significant deviations from bulk characteristics. Experimental techniques such as neutron inelastic scattering and Raman scattering of x-rays are pivotal in determining the dispersion relations of lattice vibrations within the bulk, while electron-energy loss spectroscopy and inelastic helium atom scattering are instrumental in probing the surface phonons.

Thermal neutrons, with energies commensurate with lattice vibrations and wavelengths akin to crystal lattice spacing, are adept at capturing phonon dispersion relations through the analysis of neutron scattering energy and direction. Owing to their minimal interaction with matter, they provide deep insights into the bulk phonon-dispersion patterns.

Moreover, the specific heat represents a critical material property reflecting the capacity for thermal energy storage and conduction within a solid, occurring predominantly through electronic or phonon pathways. Our focus is confined to the phonon contributions, which are crucial for understanding thermal energy management in solids. Discussions henceforth will centre on the specific heat at constant volume—a parameter of fundamental importance for solid-state physics. The vibrational specific heat pertains to the variations in energy density correlated with the lattice vibrations as a function of temperature, encapsulating the aggregate energy contributions of the system's particles.

REFERENCES

1. T. Wei, J. Wang, and D. W. Goodman, *J. Phys. Chem. C*, **111**: 8781 (2007).
2. W. Fei, A. Kara, and T. S. Rahman, *Phys. Rev. B*, **61**: 16105 (2000).
3. Y. Lu, M. Przybylski, W. H. Wang, L. Yan, Y. Shi, J. Barthel, and J. Kirschner, *J. Appl. Phys.*, **101**: 103901 (2007).
4. I. Wilkinson, R. J. Hughes, Z. Major, S. B. Dugdale, M. A. Alam, E. Bruno, B. Ginatempo, and E. S. Giuliano, *Phys. Rev. Lett.*, **87**: 216401 (2001).
5. I. Yu. Sklyadneva, G. G. Rusina, and E. V. Chulkov, *Phys. Rev. B*, **68**: 045413

(2003).
6. M. L. Grant, B. S. Swartzentruber, N. C. Barteltand, and J. B. Hannon, *Phys. Rev. Lett.*, **86**: 4588 (2001).
7. A. de Siervo, E. A. Soares, R. Landers, and G. G. Kleiman, *Phys. Rev. B*, **71**: 115417 (2005).
8. O. Skibbe, K. Berge, G. Meister, and A. Goldmann, *Phys. Rev. B*, **66**: 235418 (2002).
9. R. Xu, S. Bao, and G. Liu, *Surf. Sci.*, **234**, Iss. 3: 335 (1990).
10. S. Piccinin, C. Stampfl, and M. Scheffler, *Phys. Rev. B*, **77**: 075426 (2008).
11. A. Valcarcel, D. Loffreda, F. Delbecq, and L. Piccolo, *Phys. Rev. B*, **76**: 125406 (2007).
12. P. Delichère and J. C. Bertolini, *Surf. Interface Analysis*, **34**, Iss. 1: 116 (2002).
13. M. Abel, Y. Robach, and L. Porte, *Surf. Sci.*, **498**, Iss. 3: 244 (2002).
14. S. V. Eremeev, G. G. Rusina, and E. V. Chulkov, *Surf. Sci.*, **601**, Iss. 17: 3640 (2007).
15. J. Sun, J. B. Hannon, G. L. Kellogg, and K. Pohl, *Phys. Rev. B*, **76**: 205414 (2007).
16. L. Li, K. Xun, Y.-M. Zhou, D.-S. Wang, and S.-C. Wu, *Phys. Rev. B*, **71**: 075406 (2005).
17. N. P. Blanchard, D. S. Martin, A. M. Davarpanah, S. D. Barrett, and P. Weightman, *phys. status solidi (a)*, **188**, Iss. 4: 1505 (2001).
18. R. A. Bennett, S. Poulston, N. J. Price, J. P. Reilly, P. Stone, C. J. Barnes, and M. Bowker, *Surf. Sci.*, **433–435**: 816 (2002).
19. P. W. Murray, S. Thorshaug, I. Stensgaard, F. Besenbacher, E. Lægsgaard, A. V. Ruban, K. W. Jacobsen, G. Kopidakis, and H. L. Skriver, *Phys. Rev. B*, **55**, Iss.3: 1380 (1997).
20. T. E. Feuchtwang, *Phys. Rev.*, **155**: 731 (1967).
21. J. Szeftel and A. Khater, *J. Phys. C: Solid State Phys.*, **20**: 4725 (1987).
22. A. Khater, O. Rafil, Y. Labaye, and Y. Pennec, *Solid State Comm.*, **87**, Iss. 1: 53 (1993).
23. A. Virlouvet, H. Grimech, A. Khater, Y. Pennec, and K. Maschke, *J. Phys.: Cond. Matter*, **8**: 7589 (1996).
24. R. Tigrine, A. Khater, M. Belhadi, and O. Rafil, *Surf. Sci.*, **580**, Iss. 1–3: 1 (2005).
25. B. Bourahla, A. Khater, and R. Tigrine, *Thin Solid Films*, **517**, Iss. 24: 6857 (2009).
26. A. A. Maradudin, R. F. Wallis, and L. Dobrzynski, *Handbook of Surfaces and Interfaces* (New York: Garland STPM Press: 1980).
27. H. Grimech and A. Khater, *Surf. Sci.*, **323**, Iss. 3: 198 (1995).
28. E. A. Wimmer, *Nature Biotechnology*, **23**: 432 (2005).
29. E. J. Wu, G. Ceder, and A. van de Walle, *Phys. Rev. B*, **67**: 134103 (2003).
30. I. Y. Sklyadneva, G. G. Rusina, and E. V. Chulkov, *Phys. Rev. B*, **68**: 045413 (2003).
31. L. Li, K. Xun, Yu.-M. Zhou, D.-S. Wang, and S.-C. Wu, *Phys. Rev. B*, **71**: 075406 (2005).
32. A. Khater, R. Tigrine, and B. Bourahla, *phys. status solidi (b)*, **246**, Iss. 7: 1614 (2009).
33. A. Kara, S. Durukanoglu, and T. S. Rahman, *Phys. Rev. B*, **53**: 15489 (1996).
34. S. Iikubo, H. Ohtani, and M. Hasebe, *Mater. Trans.*, **51**, Iss. 3: 574 (2010).

35. H. L. Yu, G. W. Yang, Y. Xiao, X. H. Yan, Y. L. Mao, Y. R. Yang, and Y. Zhang, *Chem. Phys. Lett.*, **417**, Iss. 1–3: 272 (2006).
36. I. Atanasov and M. Hou, *phys. status solidi (c)*, **7**, Iss. 11–12: 2604 (2010).
37. W. Fei, A. Kara, and T. S. Rahman, *Phys. Rev. B*, **61**: 16105 (2000).
38. H. Beckmann and G. Bergmann, *Phys. Rev. Lett.*, **85**: 1584 (2000).
39. N. W. Ashcroft and N. D. Mermin, *Physique des Solides* (Paris: 2002) (in French).
40. H. T. Diep, *Physique de la Matière Condensée* (Paris: 2003).
41. C. Ngô and H. Ngô, *Physique Statistique* (Paris: 2007).
42. S. Vauclair, *Eléments de Physique Statistique* (Paris: 1993).
43. T. S. Rahman, J. D. Spangler, and A. Al-Rawi, *J. Phys.: Condens. Matter*, **14**: 5903 (2002).
44. H. Yildirim, A. Kara, and T. S. Rahman, *J. Phys.: Condens. Matter*, **21**: 084220 (2009).
45. S. Durukanoğlu, A. Kara, and T. S. Rahman, *Phys. Rev. B*, **67**: 235405 (2003).
46. T. S. Chen, G. P. Alldredge, and F. W. De Wette, *Surf. Sci.*, **62**, Iss. 2: 675 (1977).
47. H. Yildirim, A. Kara, S. Durukanoğlu, and T. S. Rahman, *Surf. Sci.*, **600**, Iss. 2: 484 (2006).
48. J. Hertz, *J. Phys. IV France*, **122**: 3 (2004).
49. L. Dobrzynski and J. Friedel, *Surf. Sci.*, **12**, Iss. 3: 469 (1968).